

# Foot Trajectory Planning Method with Adjustable Parameters for Complex Environment

Cong Zhang and Honglei An and Qing Wei and Hongxu Ma

*Department of Intelligent Robotics  
National University of Defense Technology  
Changsha Hunan Province, China  
814170070@qq.com*

**Abstract**— In order to ensure a stable and continuous walking of the quadruped robot in complex environment, a low impact foot trajectory planning method for walk gait is proposed. Firstly, a four-legged robot single-leg model with three active degrees of freedom and one passive degree of freedom is constructed. The kinematics analysis is carried out, and the foot trajectory tracking controller based on motion space is designed. Then the single-leg motion of the robot in complex environment is analysed, and the foot trajectory based on the 3rd-order bezier curve satisfying the obstacle condition is proposed. After that the method of parameter determination is further clarified. In order to reduce the impact force between the foot and the ground, the sigmoid function is introduced to process the foot trajectory. The simulation results show that through the improved bezier method, the impact between the foot and the ground can be effectively reduced.

**Index Terms**— quadruped robot, foot trajectory, complex environment, walk gait

## I. INTRODUCTION

After years of research, the application fields of mobile robots are becoming more and more extensive. According to the movement mode, the mobile robot is mainly divided into wheel type, crawler type and foot type. Compared with wheeled and crawler robots, foot robots have the characteristics of discontinuous support and are more adaptable in complex terrain and unstructured environments[1]. Among the foot robots, the quadruped robot is superior to the biped robot in stability and load capacity, and is superior to the hexagon and octagonal robots in complexity. It has become a hot spot in the research of foot robots in recent years.

The realization of foot robots in complex environments requires planning a series of discrete landing points. The realization of landing discrete points depends mainly on the planning of the robot's foot trajectory. Reasonable foot trajectory planning can not only ensure that the robot legs avoid various obstacles during the swinging process, but also reduce the impact force when the foot touches the ground. And this is critical to the stable walking of the robot. Foot trajectory planning generally needs to meet the following conditions: (1) each joint has no large impact, and the impact is small when lifting the leg and landing; (2) the trajectory of the foot end is smooth, the joint speed and acceleration

are continuously without distortion; (3) avoid the foot end sliding when in contact with the ground.

A lot of research has been done on the foot trajectory planning of foot robots. Kim K Y et al. proposed an elliptical trajectory generation algorithm for gallop gait[2]. Wilson et al. designed a new elliptical foot trajectory based on the movement of the cheetah[3]. Sakakibara et al. proposed a foot trajectory planning algorithm based on compound cycloid[4], which achieved zero impact on the foot and the ground. He Dong-qing et al. introduced acceleration segmentation on this basis, and derived and improved the improved compound cycloidal foot trajectory[5]. Han Bao-ling et al. studied the foot trajectory planning of slope based on zero impact[6]. Other commonly used foot trajectories include high-order polynomials, compound polynomials, and bezier curves. The Bezier curve has the advantages of continuous derivative and local modifiability, and is widely used in space robot trajectory planning[7], and is also used for foot trajectory planning. Compound cycloid and polynomial trajectories can better meet the requirements of small impact, but mainly used in structured environments. In complex environments, the adaptability is insufficient and it is difficult to adjust in real time. The bezier curve has strong environmental adaptability due to its ability to adjust the intermediate anchor point, but there is a large impact between the foot and the ground.

In view of the various shortcomings of the above-mentioned foot trajectory, an improved bezier curve is designed by introducing adjustable parameters. By introducing adjustment parameters, the impact of the foot end and the ground is reduced while ensuring a strong environmental adaptability of the bezier curve. The effectiveness of designing the foot trajectory by this method is verified by the simulation of the designed four-legged robot single-leg model.

## II. ROBOT MODEL ESTABLISHMENT AND KINEMATICS ANALYSIS

### A. MECHANICAL STRUCTURE OF THE ROBOT

According to the research content, a single-leg model with three active degrees of freedom and one passive degree of freedom is designed. The prototype leg and simulation model

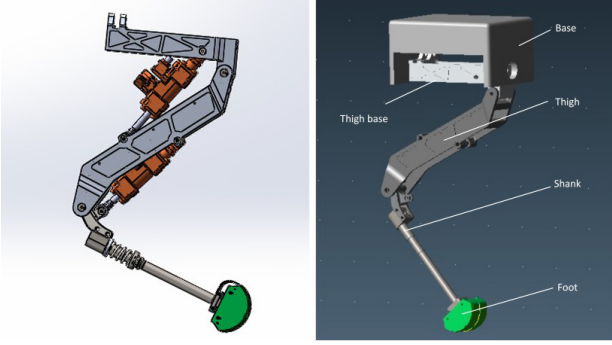


Fig. 1. Robot single-leg mechanical structure.

are shown in Fig 1, where the prototype leg is designed by SolidWorks software. In order to facilitate the development of the simulation experiment, the necessary simplification of the model is performed. The single-leg base is added and the non-essential components in the mechanical structure are simplified. The simplified model mainly includes the following parts: the body base, the thigh base, the thigh, the shank, and the semicircular foot end.

### B. KINEMATIC ANALYSIS

According to the designed quadruped robot single-leg model, the transition coordinate system from the center of body to the foot end is established, which  $\{O_G\}$  is the inertial coordinate system,  $\{O_b\}$  is the body base fixed coordinate system,  $\{O_{foot}\}$  is the contact coordinate system between the foot end and the ground, and  $\{O_1\} - \{O_4\}$  are the intermediate coordinates established by the D-H parameter method, as following Fig 2.

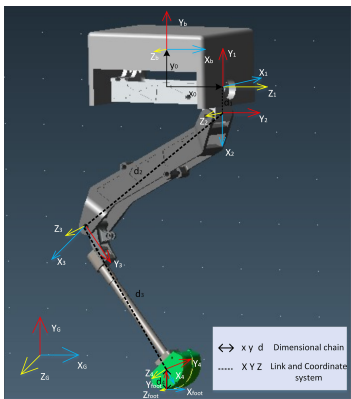


Fig. 2. One-leg model coordinate system.

The parameters of each coordinate system are given in Table 1.

TABLE I  
COORDINATE CONVERSION CARAMETER TABLE

Coordinate Transformation				
Coordinate transformation	Transformation relationship	value	Transformation relationship	value
$\{O_G\} \rightarrow \{O_1\}$	Parallel	$(x_0, y_0, 0)$	Rotate	$R_y(\pi/2)$
$\{O_4\} \rightarrow \{O_{foot}\}$	Rotate	$R_z(\xi)$	Parallel	$(0, d_4, 0)$
D-H Parameter Table				
Coordinate transformation	$\theta$	$d$	$a$	$\alpha$
$\{O_1\} \rightarrow \{O_2\}$	$\theta_1$	0	$d_1$	$\pi/2$
$\{O_2\} \rightarrow \{O_3\}$	$\theta_2$	0	$d_2$	0
$\{O_3\} \rightarrow \{O_4\}$	$\theta_3$	0	$d_3$	0

Note:  $\xi = \pi/2 - \theta_2 - \theta_3$ .

Using the conversion relationship between the coordinate systems, the translation transformation matrix is

$$T(x, y, z) = \begin{bmatrix} 1 & 0 & 0 & x \\ 0 & 1 & 0 & y \\ 0 & 0 & 1 & z \\ 0 & 0 & 0 & 1 \end{bmatrix} \quad (1)$$

and the rotating transformation matrix is

$$R_y(\alpha) = \begin{bmatrix} \cos \alpha & 0 & \sin \alpha & 0 \\ 0 & 1 & 0 & 0 \\ -\sin \alpha & 0 & \cos \alpha & 0 \\ 0 & 0 & 0 & 1 \end{bmatrix} \quad (2)$$

The D-H coordinate system transformation formula is as

$$T = \begin{bmatrix} \cos \theta & -\cos \alpha \sin \theta & \sin \alpha \sin \theta & a \cos \theta \\ \sin \theta & \cos \alpha \cos \theta & -\sin \alpha \cos \theta & a \sin \theta \\ 0 & \sin \alpha & \cos \alpha & d \\ 0 & 0 & 0 & 1 \end{bmatrix} \quad (3)$$

Let the conversion of the coordinate system  $m$  to the coordinate system  $n$  be  $T_{mn}$ . The body center to the foot end is transformed into

$$T_{body \cdot foot} = T_{body1} \cdot T_{12} \cdot T_{23} \cdot T_{34} \cdot T_{4 \cdot foot} \quad (4)$$

Bring the parameters in the Table 1 into the transformation formula, the kinematics of the single-leg can be finally obtained as

$$\begin{cases} P_x = d_3 S_{12} + d_2 S_2 + x_0 \\ P_y = S_1 (d_1 + d_4 + d_3 C_{23} + d_2 C_2) + y_0 \\ P_z = -C_1 (d_1 + d_4 + d_3 C_{23} + d_2 C_2) \end{cases} \quad (5)$$

while  $\sin(\theta_2 + \theta_3)$  is recorded as  $S_{12}$ ,  $\cos(\theta_2)$  is recorded as  $C_2$ , and the other expressions are the same. The inverse kinematics solution can be obtained by analytical method, as

$$\begin{cases} \theta_1 = \arccot(-P_z/P_y) - \pi \\ \theta_2 = -\arccos((k^2 + P_x^2 + d_2^2 - d_3^2)/2d(k^2 + P_x^2)^{1/2}) + \eta \\ \theta_3 = \arccos((k^2 + P_x^2 - d_2^2 - d_3^2)/2d_2 d_3) \end{cases} \quad (6)$$

while  $k = (P_y^2 + P_z^2)^{1/2} - d_1 - d_4$ ,  $\eta = \arctan(P_x/k)$ .

### C. CONTROLLER DESIGN FOR FOOT TRAJECTORY

According to the robot model, the PD controller shown in Fig 3 is designed to track the foot trajectory of the single leg. Matlab and Recurdyn are used for cooperative simulation to analyse the impact force of the foot end and the ground, and verify the effectiveness of the designed foot trajectory.

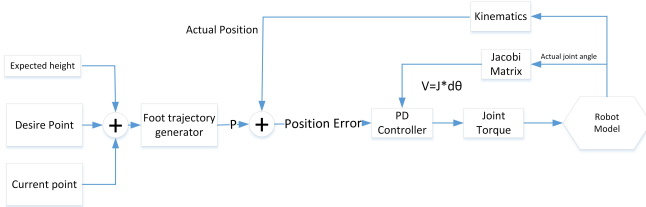


Fig. 3. PD controller design.

## III. FOOT TRAJECTORY PLANNING

### A. BEZIER CURVE TRAJECTORY PLANNING ADAPTED TO COMPLEX ENVIRONMENTS

In the natural environment, the main gait of a quadruped animal mainly includes walk, pace, bound and gallop. In order to improve the adaptability of robots in complex environments, walk gait are generally used. Robot landing point and the obstacle information in the environment are obtained by the sensor or externally. When planning the foot trajectory, it is assumed that the landing point and the obstacle information are known during swinging, and the obstacle satisfies the traversable condition. The bezier curve used in the planning is a typical interpolation curve algorithm. Because of its simple control and strong description ability, it is widely used in the field of computer graphics. During the foot trajectory planning, considering the requirement of acceleration smoothing, at least need to choose a third-order bezier curve. The zero-impact foot trajectory of Qi Na designed uses the 11-order bezier curve [8], which not only makes the selection of the intermediate point difficult, but also difficult to adapt to the complex environment. The piecewise bezier curve designed by Tan Yong-ying et al. according to the starting angle and the landing angle is difficult to meet the zero impact requirement [9].

The foot trajectory of the robot is separately planned according to the swing period and the support period. This paper focuses on the trajectory of the swing period, and the choice of the footing point is given by the upper algorithm. The 3rd-order bezier curve is selected as the basis of the foot trajectory planning during the swing period. The curve is shown in Fig 4.

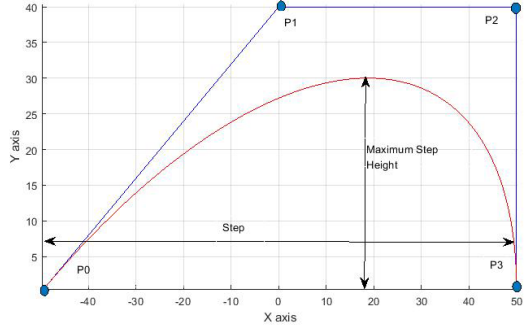


Fig. 4. The 3rd-order bezier curve foot trajectory.

The equation of any point on the curve is described as

$$P(m) = (1 - m)^3 P_0 + 3m \cdot (1 - m)^2 P_1 + 3m^2 \cdot (1 - m) P_2 + m^3 P_3 \quad (7)$$

While  $m$  is the control parameter,  $m \in [0, 1]$ .  $P_0$  represents the initial position of the swing period, and  $P_1 P_2$  represents the intermediate control point,  $P_3$  represents the desired landing point. For the convenience of analysis, we only consider the trajectory of the foot and the obstacle in the  $XOY$  plane. Assuming that the control points  $P_1$  and  $P_2$  have the same height  $H$ . The coordinates of the highest point of the curve can be calculated using (7), as

$$\begin{aligned} X_{P_{peak}} &= 3(X_{P1} + X_{P2})/8 \\ Y_{P_{peak}} &= 3H/4 \end{aligned} \quad (8)$$

Assume that the obstacle is known in the swing period, as shown by the shading in Fig 5. The black rectangular frame is drawn according to the boundary of the obstacle, and  $O_1 O_2$  are two top endpoints. When the two control points  $P_1 P_2$  are above  $\overline{P_0 P_3}$ , the 3rd-order bezier curve is a convex function, and any point on the curve is located above the string  $\overline{P_0 P_1}$  and  $\overline{P_2 P_3}$ .

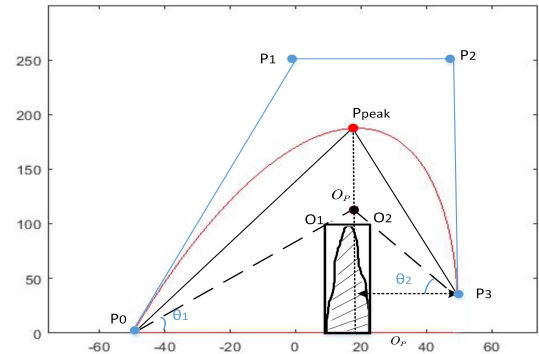


Fig. 5. The 3rd-order bezier curve foot trajectory.

Points in the Fig 5 satisfies the following relationship

$$\begin{cases} Y_{OP} \cot(\theta_1) + (Y_{OP} - Y_{P3}) \cot(\theta_2) = X_{P3} - X_{P0} \\ (X_{O1} - X_{P0}) / Y_{O1} = (X_{OP} - X_{P0}) / Y_{OP} \\ \cot(\theta_1) = (X_{O1} - X_{P0}) / Y_{O1} \\ \cot(\theta_2) = (X_{P3} - X_{O2}) / (Y_{O2} - Y_{P3}) \end{cases} \quad (9)$$

Solve the equation (9) to get the coordinates of the point  $O_p$ , as

$$\begin{cases} Y_{OP} = (X_{P3} - X_{P0} + Y_{P3} \cdot \cot(\theta_2)) / (\cot(\theta_1) + \cot(\theta_2)) \\ X_{OP} = X_{P0} + Y_{OP} \cdot (X_{O1} - X_{P0}) / Y_{O1} \\ \cot(\theta_1) = (X_{O1} - X_{P0}) / Y_{O1} \\ \cot(\theta_2) = (X_{P3} - X_{O2}) / (Y_{O2} - Y_{P3}) \end{cases} \quad (10)$$

It is known from Fig 5 that when the highest point of the selected bezier curve  $P_{peak}$  is directly above the point  $O_p$ , it can ensure that the planned foot trajectory successfully crosses the obstacle. The foot trajectory planning method of the  $YOZ$  plane is the same as above, and the point that satisfies the requirements of both the  $XOY$  plane and the  $YOZ$  plane is the final point  $O_p$ . According to coordinates of point  $O_p$ , firstly select the control point  $P_1$  on the side of the point  $O_p$ , and then find the control point  $P_1$  according to (2). When the robot is in structured environment, the parameter setting of the robot step height  $H$  can refer to the optimization method proposed by Han Bao-ling et al[10].

#### B. $\varepsilon$ – BEZIER METHOD

The 3rd-order bezier curve designed above can adjust the foot trajectory in real time according to the environmental conditions, but there is still a big impact on the ground at the moment of landing. So in order to reduce the impact, a Sigmoid function is introduced to process the trajectory. The Sigmoid function is a function commonly found in biology. It is currently used mainly as an activation function of a neural network. The discretized curve and acceleration curve are shown in Fig 6. The derivative has the characteristics of small at both ends and large in the middle, and the high-order continuous guide can well meet the speed requirement of the foot trajectory curve.

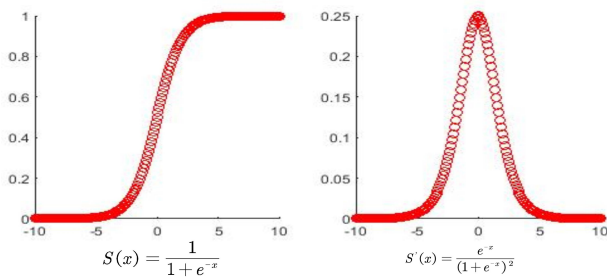


Fig. 6. Discretized sigmoid function and its derivative curve.

The bezier trajectory control parameter determined by equation (1),  $m \in [0, 1]$ , but the range of the Sigmoid function is the open interval  $(0, 1)$ . Introduce the truncation parameter  $\varepsilon$  ( $\varepsilon > 0$ ) and intercept the middle part of the Sigmoid function as Fig 7. Applying transformation (11) to the interception section can transform the amount of time to control amount that satisfies the requirements.

$$\begin{aligned} m &= (\exp(\varepsilon) + 1) / (\exp(\varepsilon) - 1) \\ &\times (1 / (\exp[-2\varepsilon(t - 1/2)] + 1) - 1 / (\exp(\varepsilon) + 1)) \end{aligned} \quad (11)$$

While  $t$  is the amount of time normalized to the swing period, and  $m$  is the control parameter of the bezier foot trajectory.

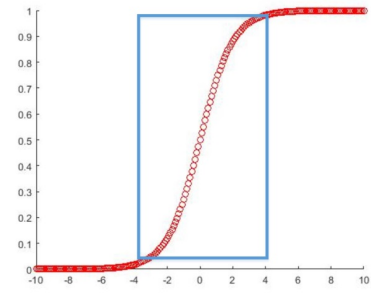


Fig. 7. Bezier curve truncation window.

The discretized foot trajectory and velocity curve corresponding to different truncation parameters are shown in Fig 8 and Fig 9. It can be seen from the figure that the larger the value is, the smaller the corresponding speed at ends of the foot trajectory is, and the smaller the impact between foot and ground is. However, the peak value of velocity in the swing period will increase, and the required acceleration will also be larger, which is limited by the power of the robot actuator. While  $\varepsilon < 1$ , the sigmoid function is approximately linear, and the effect is not obvious.

## IV. SIMULATION AND RESULT ANALYSIS

### A. SIMULATION EXPERIMENT ON SINGLE-LEG FOOT TRAJECTORY

According to the single-leg model and controller designed in the Part II, co-simulation was performed using Matlab and Recurdyn. Since the single leg movement distinguishes the swing period and the support period, the height of the body during the swing period remains unchanged, and the body provides a certain speed from the support period. In the simulation, a horizontal movement pair is applied to the body to simulate the swing period motion. In order to simulate the force between the body and the ground during support period, according to the method proposed by Dong Jin Hyun et al., a certain osmotic displacement is applied, and the support force

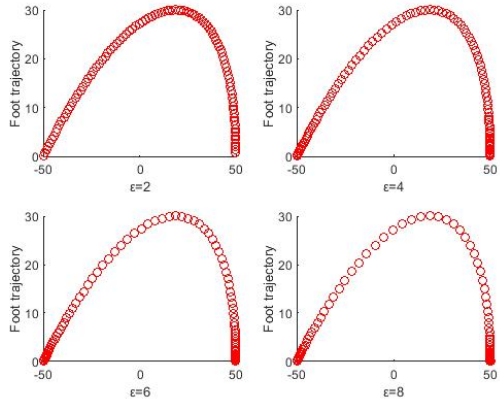


Fig. 8. Foot trajectory curve corresponding to different truncation parameters.

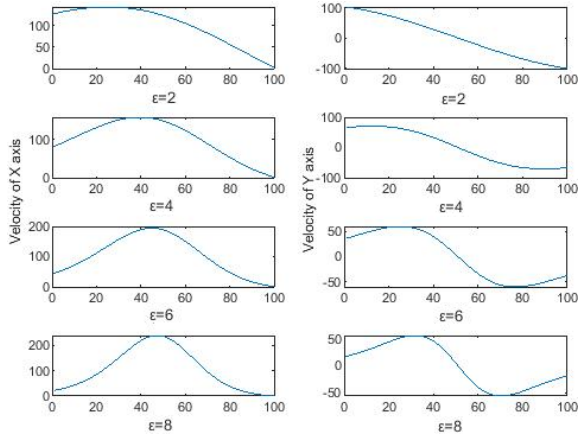


Fig. 9. Speed curve corresponding to different truncation parameters.

is characterized by the product of the osmotic displacement and the environmental stiffness[11].

The control block diagram of the system is shown in the Fig 10, which mainly includes four parts: Trajectory generator, State collector, PD controller, and Co-simulation interface. The trajectory generator part is added with parameters  $\epsilon$ , the other parameter settings are given in Table 2. A screen-shot of the co-simulation is shown in Fig 11.

TABLE II  
SINGLE-LEG SIMULATION PARAMETER TABLE

Parameters Table	
Parameters	Value(mm)
$P_0$	(-100, 0, 0)
$P_1$	(0, 120, 0)
$P_2$	(100, 120, 0)
$P_3$	(100, 0, 0)
$T$	1s

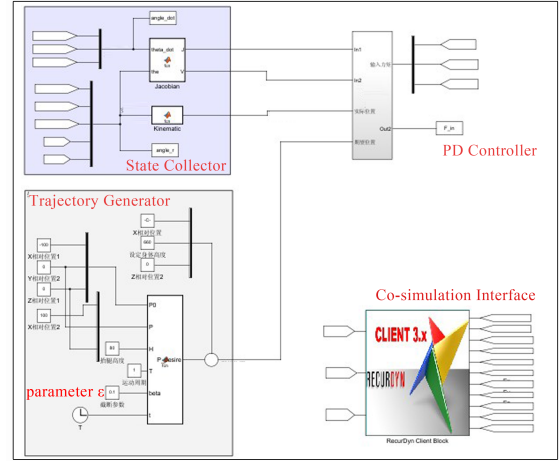


Fig. 10. Co-simulation experiment block diagram.

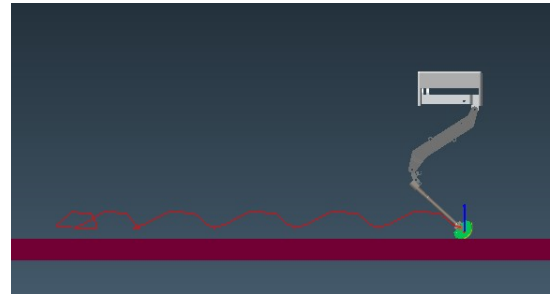


Fig. 11. Single-leg simulation screen-shot.

## B. RESULTS AND ANALYSIS

In the simulation, the speed curve of the forward direction of the body is shown in Fig 12. It can be observed from the figure that the robot accelerates from the stationary state in the first two cycles. The robot enters a steady state after the third cycle, and the first half of the cycle is the swing period. According to the conservation of energy, the forward swing of the single-leg causes fluctuations in speed. Therefore, the impact force is analysed from the third cycle.

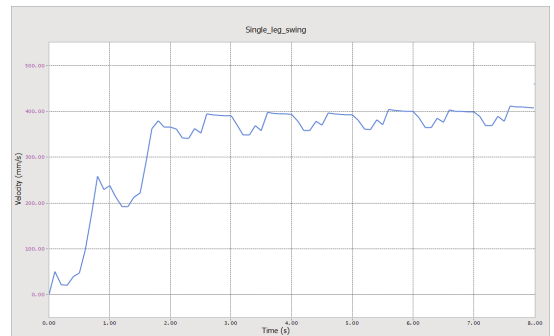


Fig. 12. Speed curve of body in the forward direction.

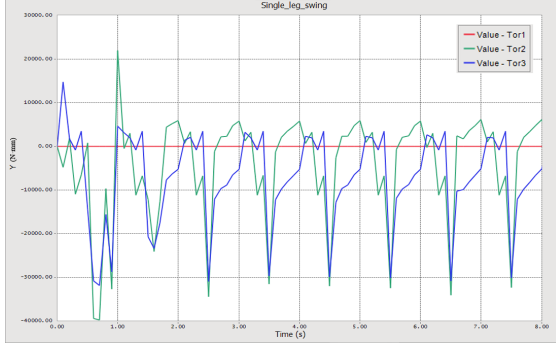


Fig. 13. Curve of input torque.

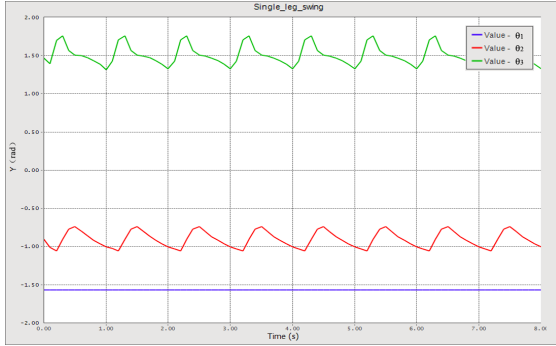


Fig. 14. Curve of joint angle.

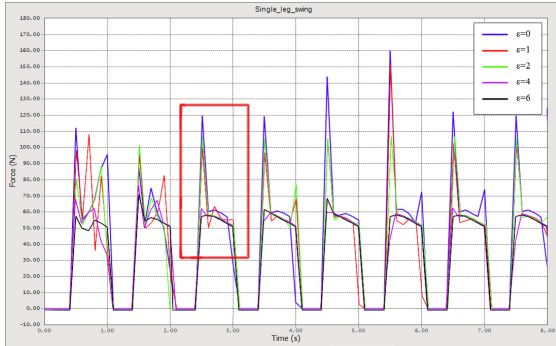


Fig. 15. Force curve between foot and ground with different parameters.

The input torque and joint angle changes in the simulation are shown in Fig 13 and Fig 14.

When the parameters  $\varepsilon$  change, the corresponding foot force curve is shown in Fig 15. The enlargement of the red box in Fig 15 is shown in Fig 16. As can be seen from the figure, compared with the ordinary bezier method, the  $\varepsilon$  - Bezier method can effectively reduce the impact force of the foot. At the same time, it is noted that when  $\varepsilon > 4$ , the impact force is basically the same as the supporting force during the support period. And while  $\varepsilon < 1$ , the effect is not obvious which verified the conclusion of the Part III of theoretical derivation.

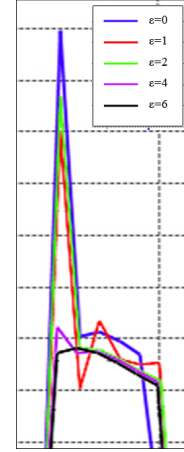


Fig. 16. The enlargement of the red box in Fig 15.

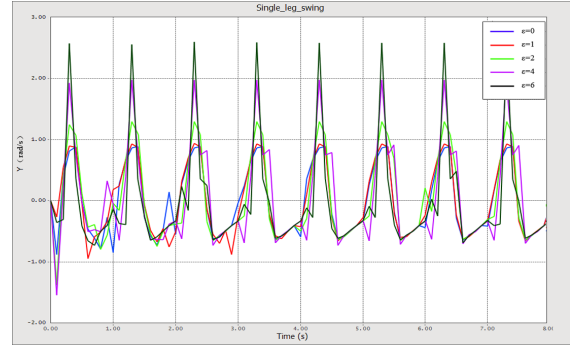


Fig. 17. The angular velocity curve of  $\theta_2$  corresponding to different parameters.

It is known from Fig 16 that increasing the parameter at this time not only has no effect, but increases the speed during the swinging process. Therefore, the value of the truncation parameter should not exceed 4, and further impact forces can be reduced by active compliance control.

## V. SUMMARY AND PROSPECT

In this paper, the foot trajectory planning is carried out based on the 3rd-order bezier curve. The obstacles in the complex environment are analysed, and proposed the method of determining control points that be able to overcome obstacles. According to the requirements of the foot trajectory of the quadruped robot, an improved method based on bezier curve is proposed, called  $\varepsilon$  - Bezier. The relative velocity between the foot and the ground is adjusted by parameters to reduce the impact force. The effectiveness of the proposed method is verified by Simulink and Recurdyn co-simulation.

However, since this paper focuses on the foot trajectory of the robot's single-leg swing period, the foot trajectory during the support period is designed to be a uniform linear motion. There is a speed mutation at the beginning and end of the support period, causing speed fluctuations during the

movement of the single-leg. Further work can use the biped or quadruped robot model to increase the support period control and form a complete robot foot trajectory planning.

#### REFERENCES

- [1] SEMINI C, TSAGARAKIS N G, GUGLIELMINO E. Design of HyQ-a hydraulically and electrically actuated quadruped robot[J]. Proceedings of the Institution of Mechanical Engineers, 2011, 225(6): 831-849.
- [2] Kim K Y, Park J H. Ellipse-based leg-trajectory generation for galloping quadruped robots[J]. Journal of Mechanical Science & Technology, 2008, 22(11): 2099-2106.
- [3] Wilson A M, Lowe J C, Roskilly K, et al. Locomotion dynamics of hunting in wild cheetahs[J]. Nature, 2013, 498(7453): 185-189.
- [4] Sakakibara Y, Kan K, Hosoda Y, et al. Foot trajectory for a quadruped walking machine[C]. IEEE International Workshop on Intelligent Robots & Systems 90 Towards A New Frontier of Applications, 1990.
- [5] HE Dong-qing, MA Pei -sun. Simulation of Dynamic Walking of Quadruped Robot and Analysis of Walking Stability[J]. Computer Simulation, 2005, 22(2): 146-149.
- [6] HAN Bao-ling, JIA Yan, LI Hua-shi, et al. Posture Adjustment for Quadruped Robot Trotting on a Slope[J]. Transaction of Beijing Institute of Technology, 2016, 36(3): 242-246.
- [7] Chen Y C. Solving robot trajectory planning problems with uniform cubic B-splines[J]. Optimal Control Applications & Methods, 2010, 12(4): 247-262.
- [8] Qi Na. Research and Realization on Locomotion Control Technology of Quadruped Robot[D]. Beijing Institute of Technology, 2015.
- [9] TAN yong-ying, WANG Rui, ZHOU Hao-sen. Foot Trajectory Planning of Four-legged Mobile Platform in Complex Environment[J]. ShanDong Industrial Technology, 2015, (22): 225-227.
- [10] HAN Bao-ling, ZHU Chen, LUO Qing-sheng, et al. Key Gait Parameter Optimization for Hydraulic Quadruped Robot[J]. Transaction of Beijing Institute of Technology, 2018, 38(10): 1056-1060.
- [11] Hyun D J, Seok S, Lee J, et al. High speed trot-running: Implementation of a hierarchical controller using proprioceptive impedance control on the MIT Cheetah[J]. The International Journal of Robotics Research, 2014, 33(11): 1417-1445.